Exposure to a non-ionic surfactant induces a response akin to heat-shock apoptosis in intestinal epithelial cells: implications for excipients safety

Robert J. Cavanagh[1], Paul A. Smith[2] and Snow Stolnik[1]*

[1]Division of Molecular Therapeutics and Formulation, School of Pharmacy, University of Nottingham

[2]School of Life Science, University of Nottingham, Nottingham, United Kingdom

Corresponding author:

* Dr Snow Stolnik, PhD

School of Pharmacy, University of Nottingham, University Park, Nottingham, NG7 2RD, UK

Tel: +44 131 242 6760

Email: snjezana.stolnik@nottingham.ac.uk

KEYWORDS: non-ionic surfactant, cell membrane permeability, apoptosis, mitochondrial hyperpolarization, heat shock

Abstract

Amphipathic, non-ionic, surfactants are widely used in pharmaceutical, food, and agricultural industry to enhance product features; as pharmaceutical excipients they are also aimed at increasing cell membrane permeability and consequently improving e.g. oral drugs absorption. Here we report on the concentration- and time-dependent succession of events occurring throughout, and subsequent exposure of Caco-2 epithelium to a 'typical' non-ionic surfactant (Kolliphor® HS15) to provide a molecular explanation for non-ionic surfactant cytotoxicity. The study shows that the conditions of surfactant exposure, which increase plasma membrane fluidity and permeability, produced rapid (within 5 minutes) redox and mitochondrial effects. Apoptosis was triggered early during exposure (within 10 minutes) and relied upon an initial mitochondrial membrane hyperpolarization (5-10 minutes) as a crucial step, leading to its subsequent depolarization and caspase-3/7 activation (60 minutes). The apoptotic pathway appears to be triggered prior to substantial surfactant-induced membrane damage (observed ≥60 minutes). We hence propose that the cellular response to the model non-ionic surfactant is triggered via surfactant-induced increase in plasma membrane fluidity - a phenomenon akin to the stress response to membrane fluidization induced by heat shock - and consequent apoptosis. Therefore, the fluidization effect that confers surfactants the ability to enhance drug permeability may also be intrinsically linked to the propagation of their cytotoxicity. The reported observations have important implications for the safety of a multitude of non-ionic surfactants used in drug delivery formulations, and to other permeability enhancing compounds with similar plasma membrane fluidizing mechanisms.

Introduction

Non-ionic surfactants are widely used in pharmaceutical, food, and agricultural industries. In the pharmaceutical industry, for example, they are employed to improve drug solubility, or to enhance transepithelial drug transport and hence increase its bioavailability.[1–3] In addition to a multitude of pre-clinical studies, non-ionic surfactants, such as the alkyl glycosides, are employed in commercially available permeability enhancing formulations, including Intravil® (Aegis Therapeutics).[4] Previous studies attribute enhancement in epithelial permeability by non-ionic surfactants to increased cell membrane fluidity [2,5] and /or to formation of channels (pores) in the plasma membrane.[6] The consequences of these changes in membrane fluidity and structure further extend to changes in function of membrane bound and cytoskeletal proteins, including P-glycoprotein and F-actin, respectively, whereby at sufficiently high concentrations, destruction of plasma membrane integrity and ultimately cell lysis could occur.[7–9] Apoptotic and necrotic death pathways have both been reported to occur upon cellular exposure to non-ionic surfactants,[10–12] however little is understood about the underlying molecular mechanisms mediating these outcomes - the aspect studied in the present work.

The non-ionic, amphipathic surfactant studied here is composed of polyoxyethylene esters of 12-hydroxystearic acid (marketed as Kolliphor® HS15, previously known as Solutol® HS15), and is used in various pharmaceutical applications including formulation of emulsions, [13,14] nanoparticles,[15,16] and as the primary component of permeability enhancing formulations.[17–19] It has a critical micellar concentration (CMC) between 0.06 - 0.1 mM, a concentration range above which it was shown to enhance bioavailability of co-administered biotherapeutic compounds across epithelial cell barrier.[8,17,18,20,21] This effect has been attributed to the surfactant's ability to increase plasma membrane fluidity, as reported for other non-ionic surfactants and indeed other

permeability enhancer compounds.[22,23] Furthermore, subsequent effects on cytoskeletal and junctional protein elements have been oberserved.[18,21] However, the effects of an increase in plasma membrane fluidity on other cell processes and cell health have not been elucidated in these studies. The present report hence focuses on deciphering the time-dependent succession of cellular events occurring in Caco-2 epithelial cells in response to their exposure to a range of the surfactant concentrations below and above the surfactant CMC. The elucidation of the mechanism of non-ionic surfactant toxicity on epithelial cells will provide vital information to enable defining exposure conditions for safe application of such compounds and aid future development of drug delivery formulations.

Materials and Methods

Cell culture

Caco-2 human colonic cancer cells were obtained from the American Type Culture Collection (ATCC; Manassas, Virginia) and were used at passages 35 – 50. Cells were cultured in EMEM (Sigma-Aldrich) supplemented with 10% (v/v) FBS (Sigma-Aldrich), 0.1 mg/ml streptomycin, 100 units/ml penicillin, 0.25 µg/ml amphotericin (Sigma-Aldrich) and 2 mM L-glutamine (Sigma-Aldrich) at 37°C with 5% CO2. Unless otherwise stated, cells were seeded at a density of 1 x 10^4 cells *per* well in 96-well plates (Corning) for 48 hours prior to assay. For the majority of assays the culture media was removed, cells washed twice with phosphate buffered saline (PBS; Sigma-Aldrich) and replaced with Kolliphor® HS15 (BASF) solutions at the required concentrations (0.01, 0.1, 1.0, 10.0, 20.0 or 50.0 mM; concentrations used were selected to be above and below the surfactant CMC [21]), or the positive control 1.0% (v/v) Triton X-100 (TX; Sigma-Aldrich). All

treatment solutions were prepared by direct solvation in Hank's Balanced Salt Solution (HBSS, pH 7.4, Sigma-Aldrich) buffered with 1% HEPES (Biochrom). The negative control in all experiments was 1% HEPES:HBSS solution.

Laurdan generalized polarization (GP)

To assess the effect of the surfactant on plasma membrane fluidity the Laurdan probe (Thermo Fisher Scientific) was employed (Sanchez et al. 2007). Cells were first incubated for 30 minutes with 2.0 µM Laurdan solution, applied in HBSS buffer at 37ºC. Fluctuations in Laurdan fluorescence were measured continuously during exposure, i.e. in the presence of surfactant solutions. Fluorescence was excited at 380 nm and emission intensity read at 440 and 490 nm (I_{440} and I_{490} respectively). Laurdan GP values were calculated by $GP = (I_{440} - I_{490})/(I_{440} + I_{490})$ as determined by Parasassi et al.[24]

LDH release assay

The lactate dehydrogenase (LDH) assay was performed according to the manufacturer's instructions (Sigma Aldrich, TOX7 kit). 75 µl *per* well of supernatant sample was removed from treated cells and transferred to a 96-well plate. 150 µl *per* well of LDH reagent was then added and the resulting mix incubated for 25 min at room temperature in the dark. Absorbance was then measured at 492 nm. Relative LDH release was calculated with the absorbance at 492 nm for untreated control cells taken as 0%, and the positive control, 1.0 % TX-100, assumed to cause total cell lysis, as 100%. This concentration of TX-100 was determined to be capable of inducing total cell lysis at exposures ≥ 5 minutes (Supplementary Figure S1).

Cellular internalization of FITC-dextran 4000 Da (FD4)

To assess the permeability of the plasma membrane to cell impermeable solutes, FITC-Dextran 4000 Da (FD4; Sigma-Aldrich) was employed as a model permeant.[25,26] Solutions containing surfactant at specified concentration and FD4 (200 µg/ml) were applied to cells for 5-240 minutes. Following exposure, cells were washed three times with PBS buffer and fluorescence measured at 490/525 nm (excitation/emission) to detect the presence of internalized FD4.

MTS assay

The cellular reduction of MTS reagent (CellTiter 96 Aqueous Cell Proliferation Assay, Promega) was assessed following surfactant exposure for predetermined times (5-240 minutes). Cells were incubated with 120 µl MTS solution (17 % v/v applied in EMEM) for 120 minutes, after which absorbance was measured at 492 nm. MTS reduction data was normalized by setting values of the untreated control cells as 1, and values from cells treated with 1% TX-100 as 0.

JC-1 assay

Changes in mitochondrial membrane potential were monitored by a JC-1 (Biotium) aggregation assay.[27] Following cells exposure to the surfactant solutions under different conditions, these were removed and cells washed twice with PBS buffer, prior to incubation with 50 µl JC-1 dye (5 µg/ml in EMEM) for 15 min at 37°C. Following removal of dye solution, wells were washed with PBS buffer prior to measuring fluorescence at 550/600 nm (excitation/emission) for detection of JC-1-aggregates, and 485/535 nm (excitation/emission) for detection of JC-1 monomers. J-aggregate:monomer ratios were then normalized to values induced by the untreated control (set to

a value of 1) and 1 µM valinomycin (Sigma-Aldrich) (set to a value of 0) was employed as a known depolarizing agent [28] (Supplementary Figure S2).

CellTox green assay

Integrity of the nuclear membrane was measured by the binding of CellTox Green (Promega) to nuclear DNA.[29] Following cells exposure to the surfactant solutions under different conditions, CellTox Green reagent (150 µl; 1:500 dilution of CellTox Green Dye in Assay Buffer) was added *per* well and the resulting solution incubated at room temperature for 15 min in the dark. Fluorescence was measured at 495/519 nm (excitation/emission). Relative CellTox Green binding DNA was calculated with the control, untreated cells (HBSS buffer containing 1% HEPES) set as 0%, and the positive control (1.0% TX-100) set as 100%.

Hoechst 33342 /propidium iodide microscopy

Integrity of the nuclear membrane and nuclear fragmentation was measured by propidium iodide (PI; Thermo Fisher Scientific) uptake.[30] $6x10^4$ Caco-2 cells *per* well were seeded in 24 well plates (Corning) and cultured for 48 hours. Wells were washed twice with PBS before addition of Kolliphor HS15 solution at the required concentration, or 100% ice cold ethanol (positive control; Fisher Chemical) for 240 minutes. Treatment solutions were then aspirated, cells washed with PBS, followed by addition of 1 µM Hoechst 33342 (Thermo Fisher Scientific) in PBS for 5 minutes and then 0.1 mg/ml propidium iodide (PI) in PBS (final concentration ~ 2 µg/ml PI) and the cells incubated for a further 5 minutes after which the solution was removed, and the cells washed with PBS. Cells were then imaged on an inverted EVOS fluorescent microscope using a DAPI filter (357/447 nm; excitation /emission) for detection of Hoechst signal, and RFP filter (531/593 nm; excitation /emission) for PI signal.

Determination of ROS induction

Intracellular ROS levels were assessed using the CM-H2DCFDA probe (Thermo Fisher Scientific).[31] After exposure to treatments, cells were loaded with 10 µM CM-H2DCFDA in HBSS for 30 minutes at 37°C. The probe was removed, cells washed, and fluorescent intensity measured at 492/520 nm (excitation /emission). Measured values were then normalized to the untreated control (set as a value of 1).

Detection of activated caspase-3/7

The CellEvent ® caspase-3/7 green detection reagent (Thermo Fisher Scientific) was employed to evaluate levels of activated caspase-3 or 7.[32] After exposure to surfactant solutions, 150 µl 2% (v/v) CellEvent probe in PBS was applied *per* well for 30 minutes at 37°C. Fluorescent intensity was measured at 502/530 nm excitation /emission) and normalized to the untreated control (set as a value of 1).

Calcium imaging

Intracellular Ca^{2+} was monitored by epifluorescent microscopy with the Ca^{2+} fluophore, FLUO-4 AM (Thermo Fisher Scientific).[33] Caco-2 cells were seeded on 15 mm borosilicate coverslips at a density of $1.2x10^5$ cells *per* well and cultured for 48 hours in complete EMEM. Cells were incubated with 1 µM FLUO-4 (in HBSS) for 30 mins, and then perifused with HBSS buffer with or without 50.0 mM Kolliphor HS15 at 32°C. Cells were imaged on an inverted Axiovert 135T*V* microscope under continual illumination at 490 nm. Cell fluorescence at >510 nm was captured with 20x magnification at 1 Hz with a Coosnap HQ2 camera (Photometrics, UK) using Imaging Workbench (Version 6, Indec).

For each visual field studied, regions of interest (ROI) were drawn around single and cluster of cells. These were corrected for background fluorescence by subtraction, and fluorescence intensity traces generated as a function over time. Image analysis was performed with custom scripts written in Labtalk (OriginLab Corporation, MA USA).

Statistical analysis

Concentration-response relationships were quantified by fitting the data with the equation:

$$R = \frac{\mathrm{Rmin} + (R_{max} - R_{min})}{1 + (\frac{[S]}{EC_{50}})^{h}}$$

where R is the response magnitude, R_{min} is the minimum value, R_{max} is the maximum value, *h* is the slope index, [S] is the surfactant concentration and EC_{50} the concentration that produces half-maximal effect.

Statistical analysis, unless otherwise stated, was performed by one-way ANOVA with Dunnett's multiple comparison *post hoc* test using GraphPad Prism (version 7.0). In the figures, statistical probability is indicated by: *, $P < 0.05$; **, $P < 0.01$; ***, $P < 0.001$; ****, $P < 0.0001$. With multiple plots the statistical significance placed close to the relevant plot, and written in a coordinated colour to the plot. All data are presented as mean ± S.D from triplicates of three independent experiments, unless stated otherwise.

Results

Surfactant exposure effect on Caco-2 cell membrane fluidity

Initially the effect of cells exposure to the non-ionic surfactant on plasma membrane fluidity was assessed using Laurdan general polarisation (GP) (Figure 1). The analysis reveals that prior to the surfactant treatments (-4 to 0 minutes), Caco-2 cells maintained in HBSS buffer had baseline GP value of 0.19 ± 0.04, in agreement to Laurdan GP value reported in the literature for this cell line. [34] Addition of the surfactant resulted in an almost immediate (evident at the first time- point of measurement, 1 minute) concentration-dependent decline in GP value for solutions at concentrations of ≥0.1 mM (Figure 1b). Following the initial decline, GP values maintained constant for at least 30 minutes for low concentration solutions (for example for ≤1.0 mM Kolliphor HS15 ΔGP for from 1-40 minutes time period was not significantly different to the buffer control (Figure 1c)), whilst higher concentrations (for example 10 mM solution) displayed a significant decay in GP over the same time period (1-40 minutes). Most prominent second decline in GP was then seen between 30-40 minutes (Figure 1c). In comparison, exposure of Caco-2 cells to 1% v/v Triton X-100 solution resulted in a significant initial decline in GP value (0-1 minutes) that was considerably larger in magnitude than for Kolliphor HS15 solutions, apart from the highest 10.0 mM concentration applied, which did not differ statistically ($P>0.05$) (Figure 1c). However, unlike Kolliphor HS15 solutions, Triton X-100 induced a gradual, significant decay in GP value between 1-40 minutes of -1.2×10^{-3} ΔGP/min (Figure 1c). GP values obtained at 90 and 180 minutes of exposure show further statistically significant decrease for solutions ≥1 mM, relative to values at 1 minute of exposure time point (Figure 1a). Thus, the Laurdan study data reveal statistically significant increase in cell membrane fluidity early on exposure to the surfactant at concentrations ≥0.1 mM, and which further increases on prolong exposure.

Figure 1d provides a comparison of Laurdan probe's behaviour when Caco-2 plasma membrane fluidization was induced by a temperature (42ºC). It shows the comparable Laurdan GP values of cells exposures to surfactant and to increased temperature (42ºC) at early time points. Cell exposure to 42ºC treatment was reported to induce an increase in cell membrane fluidity and the heat shock response.[35,36]

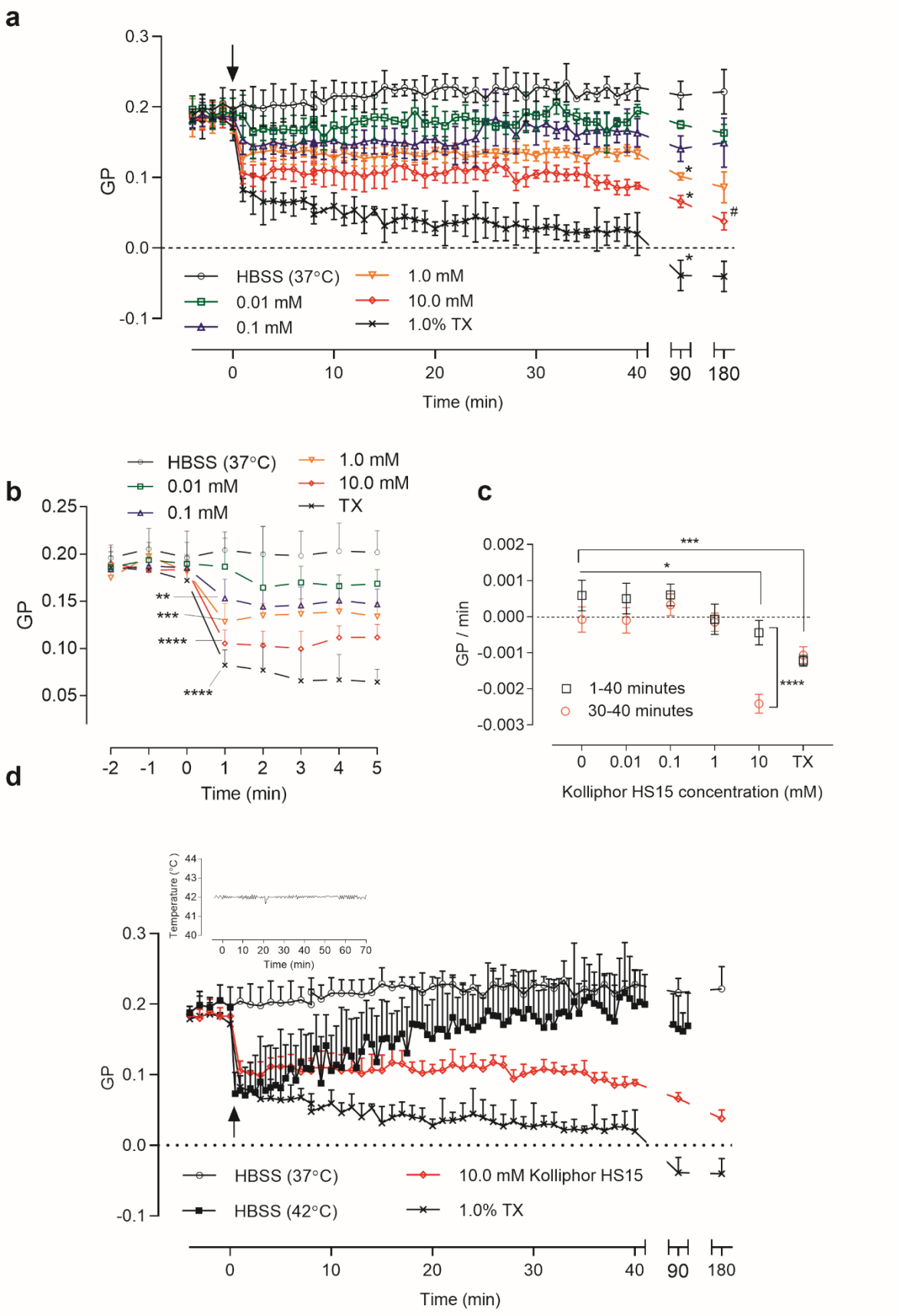
a
GP
Time (min)
HBSS (37°C)
0.01 mM
0.1 mM
1.0 mM
10.0 mM
1.0% TX
b
GP
Time (min)
HBSS (37°C)
0.01 mM
0.1 mM
1.0 mM
10.0 mM
TX
c
GP / min
1-40 minutes
30-40 minutes
Kolliphor HS15 concentration (mM)
d
Temperature (°C)
Time (min)
GP
HBSS (37°C)
HBSS (42°C)
10.0 mM Kolliphor HS15
1.0% TX
Time (min)

Figure 1. Laurdan generalised polarisation (GP) of Caco-2 cells. **(a)** Time dependency of GP in response to treatments indicated: HBSS buffer control; 0.01-10.0 mM Kolliphor HS15 and 1.0% v/v Triton X-100 (1.0% TX). Arrow indicates starting point of exposure. * signifies significant difference ($P<0.05$) between GP values measured at 1 and 90 minutes, and # signifies significance ($P<0.05$) between 90 and 180 minutes. Statistical inference between various times at the different surfactant concentrations are by 1-way ANOVA with Tukey's multiple comparison test. **(b)** Expanded time scale of GP values between -2 and 5 minutes highlights significant decreases in GP observed between 0 and 1 minute (as denoted with asterisks). **(c)** Rate of Laurdan GP change per minute (ΔGP/min) for data gathered between 1-40 and between 30-40 minutes time points. **(d)** GP measurements after heat shock (HBSS applied at 42°C). For reference, GP profiles of HBSS applied at 37°C, 10.0 mM Kolliphor HS15and TX are displayed. Insert displays average (mean) temperature of system (interior of TECAN plate reader) measured throughout repeats. Data are all shown as mean ± S.D (N=3, n=3).

Calcium flux on surfactant exposure

Figure 2 demonstrates that upon application to 50 mM surfactant solution, cells exhibit a transiently increased intracellular calcium levels within the first 20 minutes of exposure. This response is characterised by an initial peak in calcium, of approximately 5-10% of basal levels, occurring within first 3 minutes, and a subsequent decrease to basal levels between 5-20 minutes of surfactant exposure. On longer exposures (≥ 40 min), loss of Ca^{2+} homeostasis was observed in a time-dependent manner (Supplementary Figure S3).

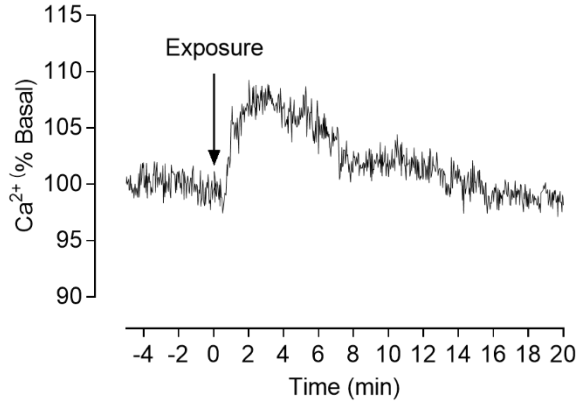

Figure 2. Intracellular calcium changes in Caco-2 cells on exposure to Kolliphor HS15. Trace displays mean result from three independent experiments, each replicate itself being the mean response of at least 15 cells. Data are normalised to the average basal signals of cells prior to Kolliphor HS15 application (-5 to 0 mins).

Surfactant influence on permeability of cellular membranes

Figure 3 summarizes the time- and concentration-dependent effects of surfactant exposure on the membrane integrity of Caco-2 cells. At the lowest concentration applied (0.01 mM) the surfactant did not affect influx of FD4 hydrophilic probe, release of cytoplasmic LDH protein, or permeability of the nuclear membrane for up to 240 minutes, the longest exposure time tested (Figure 3a). At concentrations ≥0.1 mM, the surfactant impaired cell membranes integrity; as indicated by significant release of LDH, influx of FD4 probe, and increased nuclear membrane permeability observed at 60 minutes of the exposure. Regarding permeability of nuclear membrane to CellTox green probe, staining of the cell nucleus was observed; suggesting an increased permeability of the probe into the cell and nucleus, rather than cellular leakage of DNA material (Supplementary Figure S4).

Profiles for FD4 internalization and LDH release follow similar trend, indicating that the plasma membrane permeability is generally increasing at surfactant solutions of ≥0.1 mM (Figure 3a). The release of LDH shows clear concentration dependence; after 240 minutes incubation the EC_{50} is 0.56 mM (0.3 to 1.0 mM, 95% C.I.) and h was 0.73 (0.54 to 1.0, 95% C.I) (Figure 3b). Figure 3c illustrates that the potency of the surfactant significantly increased with incubation time ($r = -0.993$, $P < 0.01$, Pearson).

It should be however noticed that at early time points, 5 and 10 minutes, cells exposure to high concentrations of the surfactant (≥10.0 mM) show a significantly lower FD4 internalization, compared to untreated control (taken as 100%) (Figure 3a).

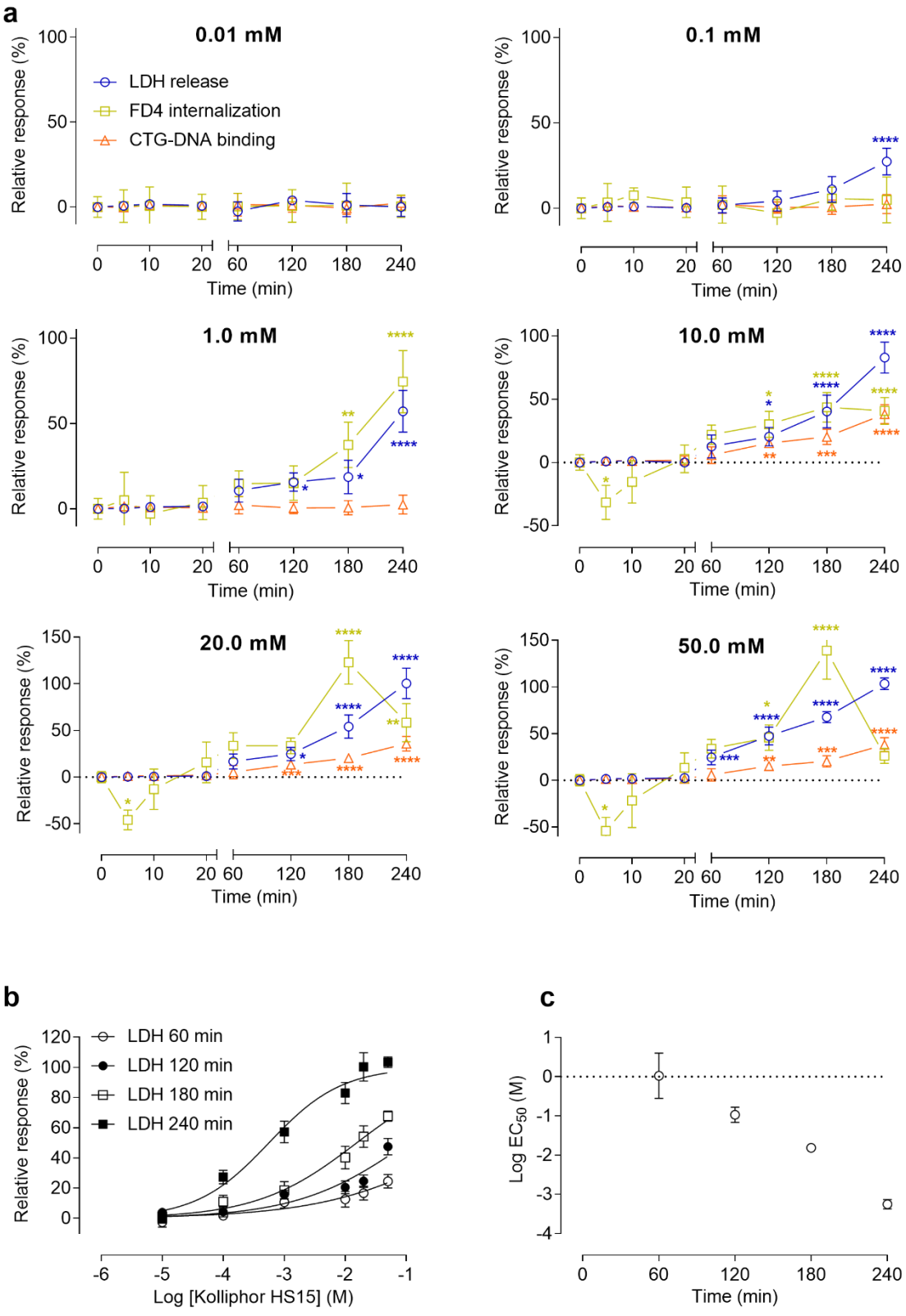
a
0.01 mM
0.1 mM
1.0 mM
10.0 mM
20.0 mM
50.0 mM
LDH release
FD4 internalization
CTG-DNA binding
Relative response (%)
Time (min)
b
LDH 60 min
LDH 120 min
LDH 180 min
LDH 240 min
Relative response (%)
Log [Kolliphor HS15] (M)
c
Log EC50 (M)
Time (min)

Figure 3. Cell membrane effects of Kolliphor HS15 on Caco-2 cells. (a) Effect of exposure to Kolliphor HS15 on Caco-2 plasma membrane permeability as indicated by the release of LDH, internalization of FD4 and, as a marker of nuclear membrane permeability, the binding of CellTox Green to DNA. Cells were exposed for increasing concentrations of the surfactant as indicated. **(b)** Concentration-effect relationship for the effect of Kolliphor HS15 on LDH release at different exposure times. Solid lines are fitted to the data by sigmoidal dose-response (variable slope) curves (GraphPad 7.0). **(c)** Relationship between Log EC50, as determined from **b**, and time of exposure. Data are mean ± S.D (N = 3, n = 3) and are displayed as the relative response to that observed with control (described in materials and methods). Statistical inference between various times for each assay are by 1-way ANOVA with Dunnett's multiple comparison test.

Surfactant effect on mitochondrial and cell metabolism

The mitochondrial effects of surfactant exposure are shown in Figure 4. As observed in Figure 3, exposure to a surfactant concentration below its CMC (0.01 mM) did not result in measurable changes in MTS reduction, mitochondrial membrane potential, or ROS levels, relative to untreated cells. However, exposures to concentrations above the CMC (≥0.1 mM) demonstrate statistically significant increases in MTS reduction, *hyperpolarization* of the mitochondrial membrane potential, and increased ROS levels at 5, 10 and 20 minutes exposure (Figure 4). Cells exposure to 1 mM H_2O_2 for 20 minutes was determined to induce a 6.5-fold increase in ROS levels (Supplementary Figure S5).

Longer exposures (≥ 60 minutes) resulted in *depolarization* of the mitochondrial membrane potential, decrease in ROS levels and decreased MTS reduction for surfactant solutions ≥1.0 mM (Figure 4). Prolonged exposure (180 and 240 minutes) caused mitochondrial depolarization and metabolic effects even for low concentrations of surfactant solution (0.1 mM) (Figure 4). It should be noted that the latter events occur in the same time frame as the membrane permeabilization illustrated in Figure 3. Responses assessed with MTS reduction based and JC-1 based

mitochondrial membrane potential assays corroborate with alternative tests, including the PrestoBlue assay (Supplementary Figure S6) and Mitotracker probe (Supplementary Figure S7), respectively.

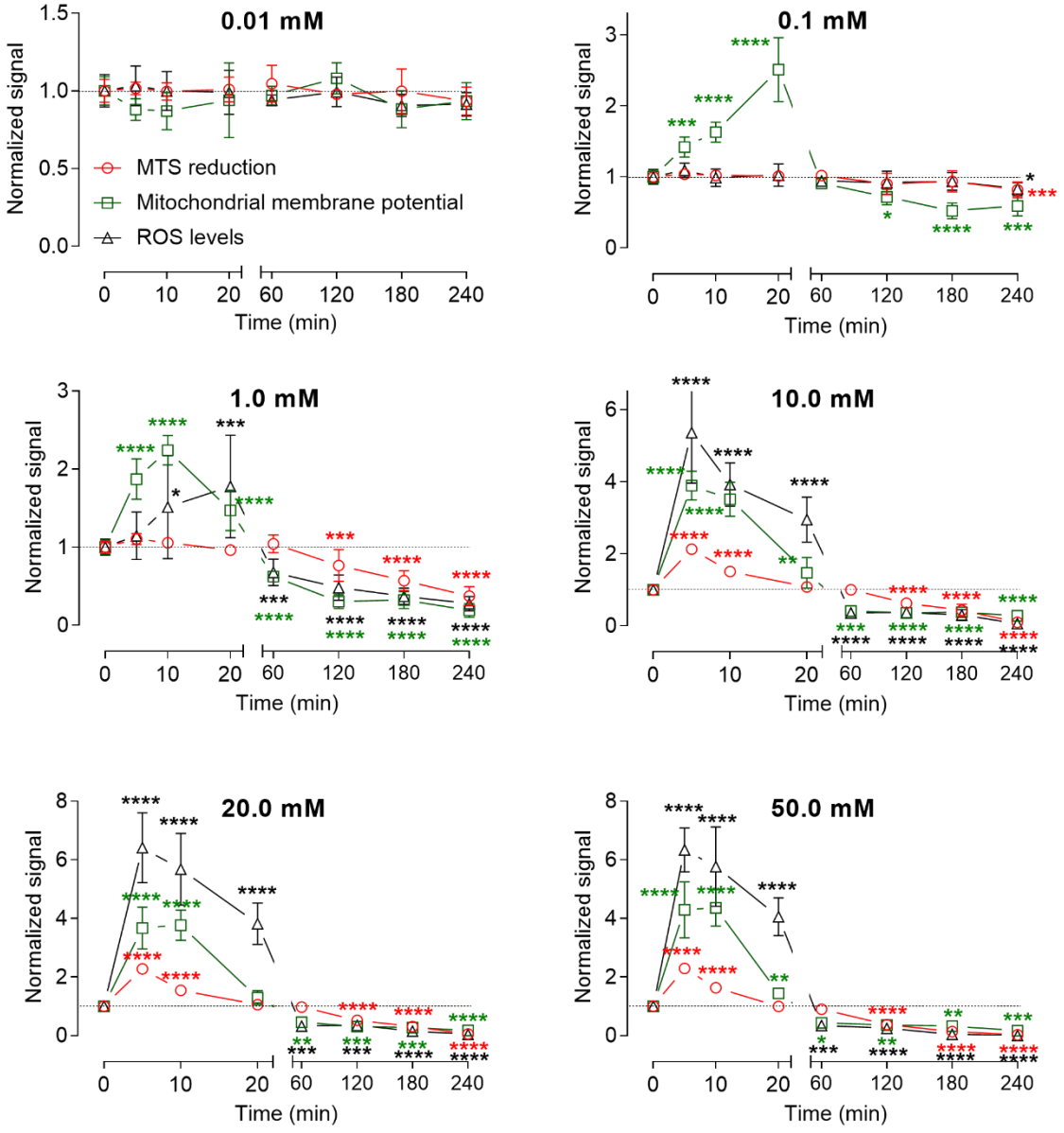

Figure 4. Effect of Kolliphor HS15 on Caco-2 mitochondrial and metabolic activity. Cells were exposed for 5-240 minutes to increasing concentrations of Kolliphor HS15 solutions as indicated. Mitochondria membrane potential was evaluated using the JC-1 assay, metabolic activity by MTS reduction and intracellular ROS levels assessed using the CM-H2DCFDA probe. Data are mean ± S.D (N = 3, n = 3) and are displayed normalized to that observed with control (described in materials and methods). Statistical inference between various times for each assay are by 1-way ANOVA with Dunnett's multiple comparison test.

Post exposure metabolic-decline and activation of effector caspases

To explore the reversibility of cellular effects to surfactant exposure, particularly reversibility of effects of short exposures (5-20 minutes), exposed cells were subjected to a 'recovery' post-exposure period and evaluated, as illustrated in Figure 5a. The MTS assay conducted at different post-exposure times reveals a general trend - as initial exposure time is increased, the emergence of metabolic decline appears at earlier post-exposure times. Regarding caspases 3 and 7, following different exposure times these were observed activated at 6 hours post surfactant exposure when surfactant concentrations of ≥1.0 mM were applied for ≥10 minutes (One way ANOVA) (Figure 5b) but, interestingly, when applied for a short period of 5 minutes a concentration-dependent decrease in caspase-3/7 activation was observed even for high surfactant solutions (1-10 mM) to values below that measured under control conditions (treatment with HBSS buffer). For reference, staurosporine (10.0 μM), a known inducer of apoptosis,[37] induced a normalized caspase 3/7 activation value of approximately 5.5-fold the negative control (Supplementary Figure S8).

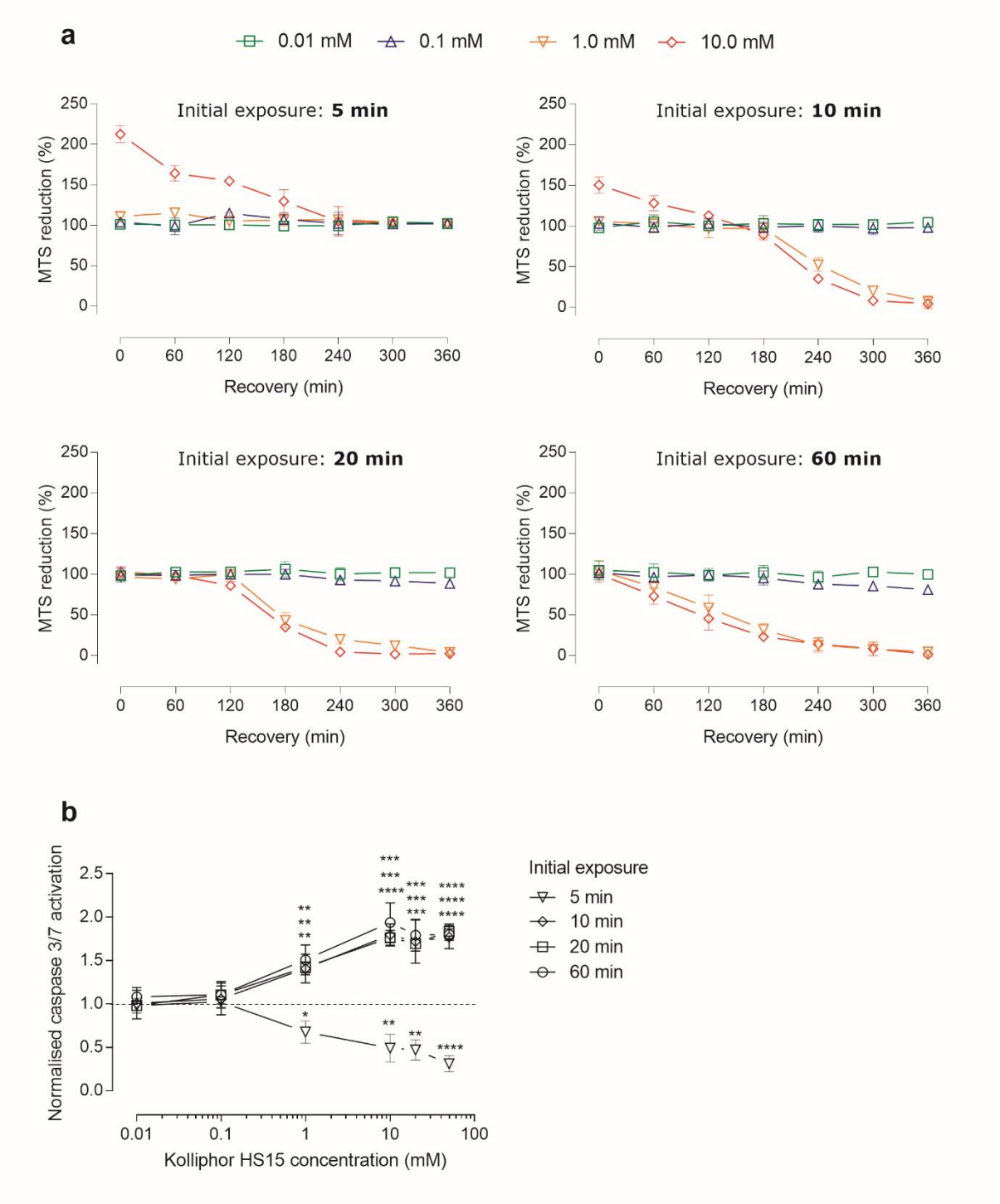

Figure 5. Post-exposure assessment of surfactant effects. (a) MTS reduction in Caco-2 cells exposed to Kolliphor HS15 (0.01-50 mM solutions) for 5, 10, 20 and 60 minutes as different post-exposure, 'recovery' times. **(b)** Concentration and time dependence of caspase-3 and 7 activation in Caco-2 cells. Cells were initially exposed to Kolliphor HS15 for 5, 10, 20 and 60 minutes and subjected to a 'recovery' period of 360 minutes in the absence of surfactant

followed by the assessment of caspase activation. Data are mean ± SD (N = 3, n = 3) and are displayed normalized to that observed with control (described in materials and methods). Statistical inference between various times at any given concentration are by 1-way ANOVA with Dunnett's multiple comparison test.

Assessment of nuclear morphology and permeability

Figure 6 presents fluorescence microscopy images of Hoechst 33342 (Ho) and propidium iodide (PI) double staining of Caco-2 nuclei. It depicts that 240 minutes exposure to 10.0 mM surfactant solution induces positive PI staining of all cells, as indicated by the purple colour of nuclei in the merged images (Ho/PI), indicating increased plasma and nuclear membrane permeability. Neither the negative (HBSS buffer) nor the positive apoptotic controls (10.0 μM staurosporine) induced PI staining (Figure 6). In some surfactant treated cells (10.0 mM, 240 minutes) the pro-apoptotic feature of nuclear fragmentation is noted, this was also evident in the staurosporine treated cells (Figure 6; inserts i and ii; indicated by white arrows). Nuclear fragmentation was not observed in the negative control or in cells exposed in the necrotic (100% ethanol) treatment group. Cells treated with the necrotic control appeared to have swollen nuclei (Figure 6; insert ii), while cell exposure to the surfactant or the apoptotic control for 240 minutes did not result in significant changes in nuclei size (Figure 6; bar chart). Figure 6 corroborates results from the DNA binding assay in Figure 3.

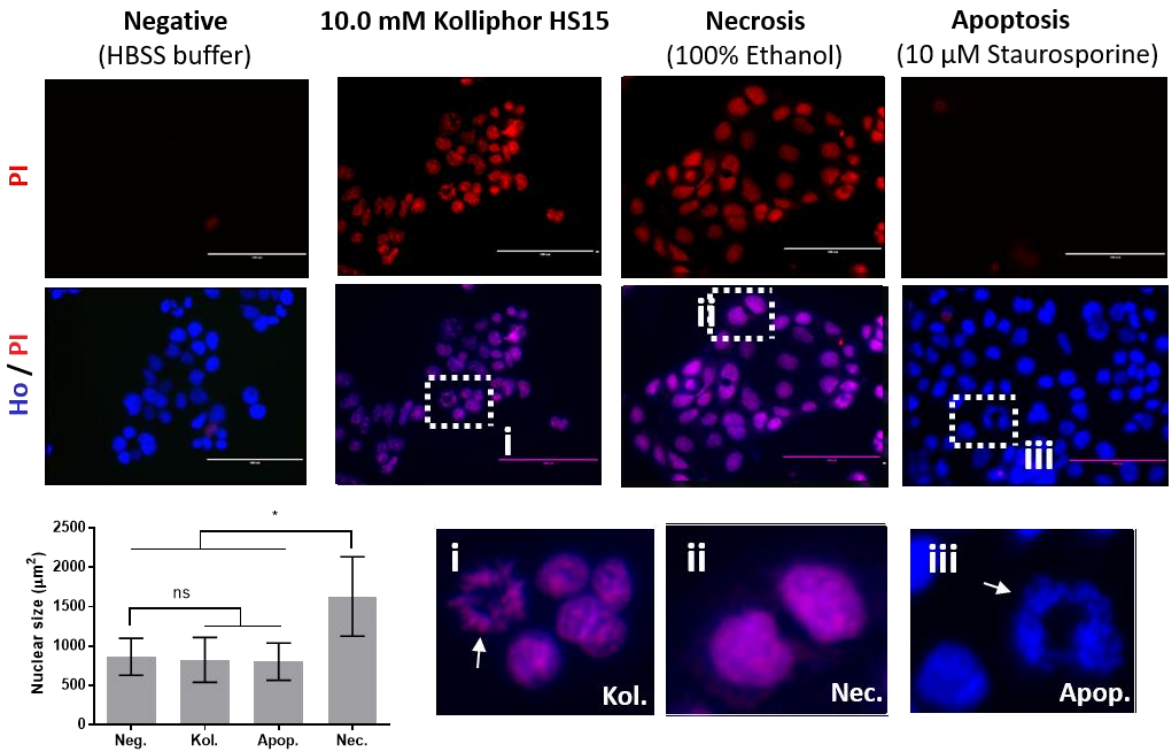

Figure 6. Hoechst 33342 and propidium iodide double staining of Caco-2 nuclei. Top row, propidium iodide (PI) staining imaged on RFP filter (λ_{ex} 531/40 nm; λ_{em} 593/40 nm). Middle row (Ho/PI) shows merged images of PI staining with Hoechst 33342 (Ho), Ho stain was imaged on DAPI filter (λ_{ex} 357/44 nm; λ_{em} 447/60 nm) and images merged using ImageJ software. Images shown are representative of 3 sets of independent images. Cells were exposed to treatments for 240 minutes and imaged on EVOS microscope 40X magnification (scale bar 100 µm). Bottom row, bar chart illustrates the mean ± S.D of nuclei size (μm^2) of treated cells (Neg, negative control; Kol., 10 mM Kolliphor HS15; Apop., 10 µM Staurosporine; Nec., Ethanol) measured using ImageJ analysis software and counting of at least 100 cells per group. Statistical significance measured using one-way ANOVA. Inserts (i, ii and iii) represent enlarged areas highlighted by white dotted boxes from Ho/PI micrographs and highlight morphological differences of nuclei between treatments. White arrows indicate nuclei with apoptotic features.

Effect of mitochondrial hyperpolarization on surfactant responses

To investigate the importance of *early* mitochondrial *hyperpolarisation*, cells were co-treated with the surfactant and a sub-toxic concentration of FCCP (0.5 µM), a mitochondrial protonophore

known to depolarize mitochondrial membrane at high (toxic) concentrations and inhibit its hyperpolarization at low concentrations.[38,39] The applied FCCP concentration (0.5 μM) did not induce mitochondrial membrane depolarization, yet was able to diminish the increase in $\Delta\Psi_m$ elicited by the surfactant (Supplementary Figure S9).

Profiles in Figure 7a illustrate that FCCP presence diminishes the early (5-20 minutes) mitochondrial membrane *hyperpolarization* induced by 0.1, 1.0 and 10.0 mM surfactant solutions. Moreover, co-treatment with FCCP conferred cells the ability to withstand longer surfactant exposures (60 and 120 minutes) prior to a decrease in mitochondrial membrane potential $\Delta\Psi_m$ (depolarization).

FCCP co-treatment also protected against the surfactant-induced decrease in cellular MTS reduction (Figure 7b), as well as increase in ROS production (Supplementary Figure S10). Importantly, FCCP suppressed the activation of caspase-3/7 at all surfactant concentrations tested up to 240 min exposure (Figure 7c). FCCP treatment did not however influence surfactant-induced increases in nuclear membrane permeability (Supplementary Figure S11).

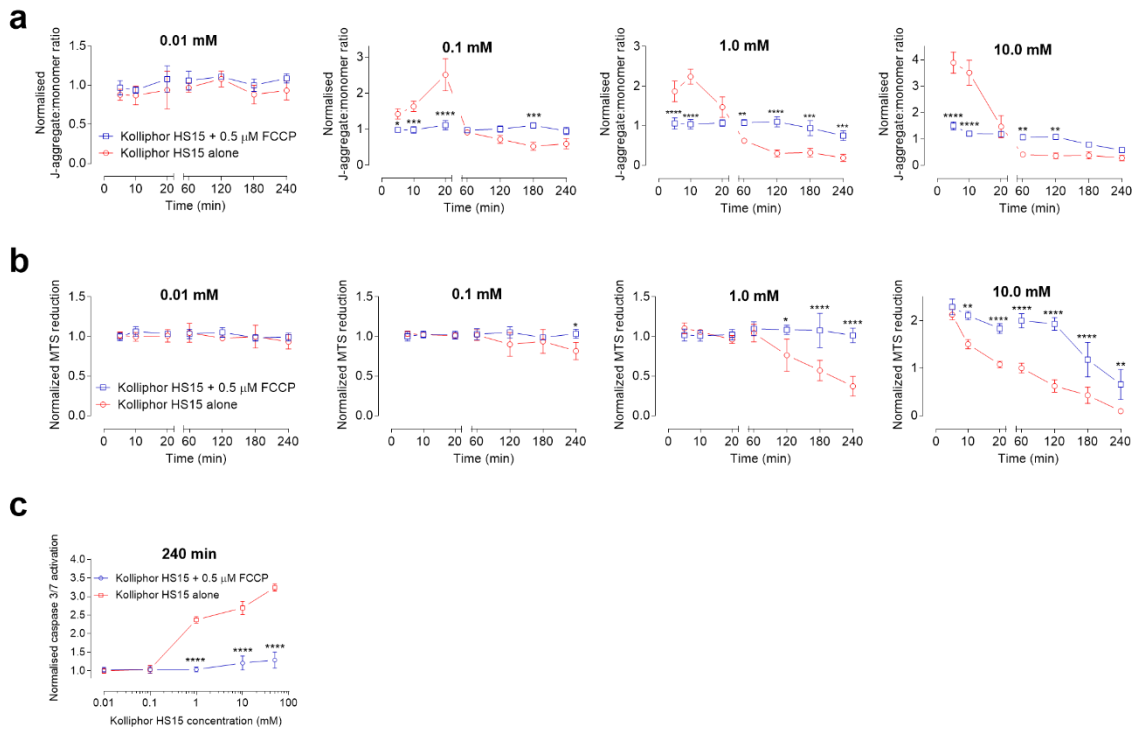

Figure 7. Effect of 0.5 µM FCCP on Kolliphor HS15 induced mitochondrial-associated effects in Caco-2 cells. Time-dependent changes in **(a)** mitochondrial membrane potential, as indicated by the ratio of J-aggregate to monomer ratio, and **(b)** MTS reduction at the concentration of surfactant indicated. **(c)** Concentration effect of Kolliphor HS15 on caspase-3/7 activation after 240 minutes exposure time. All data are presented normalised to the vehicle control (HBSS buffer). Statistical differences between Kolliphor HS15 alone and Kolliphor HS15 co-treatment with FCCP are by 2-way ANOVA with Sidak's multiple comparison test.

Discussion

The increased permeability of epithelial cell layer to different permeants (e.g. small drug molecules and biologics) induced by non-ionic surfactants used as permeability enhancers has been connected to their effects on cell plasma membranes.[2,40] However, studies to decipher the mechanism(s) by which increased membrane permeability may be connected to other cellular

events, including cytotoxicity of non-ionic surfactants are scarce.[3] In the present work we corroborate the time-dependent membrane, mitochondrial, and cell death-associated impacts of a non-ionic surfactant to develop a toxicity profile that will aid in the understanding of how these compounds can be safely utilized. Evaluating surfactant effects on cells as a function of exposure time, rather than typical measurements at a single time point, allowed us to discuss the surfactant effects in the context of time (as illustrated in Figure 8) and enable mechanistic information to be elucidated.

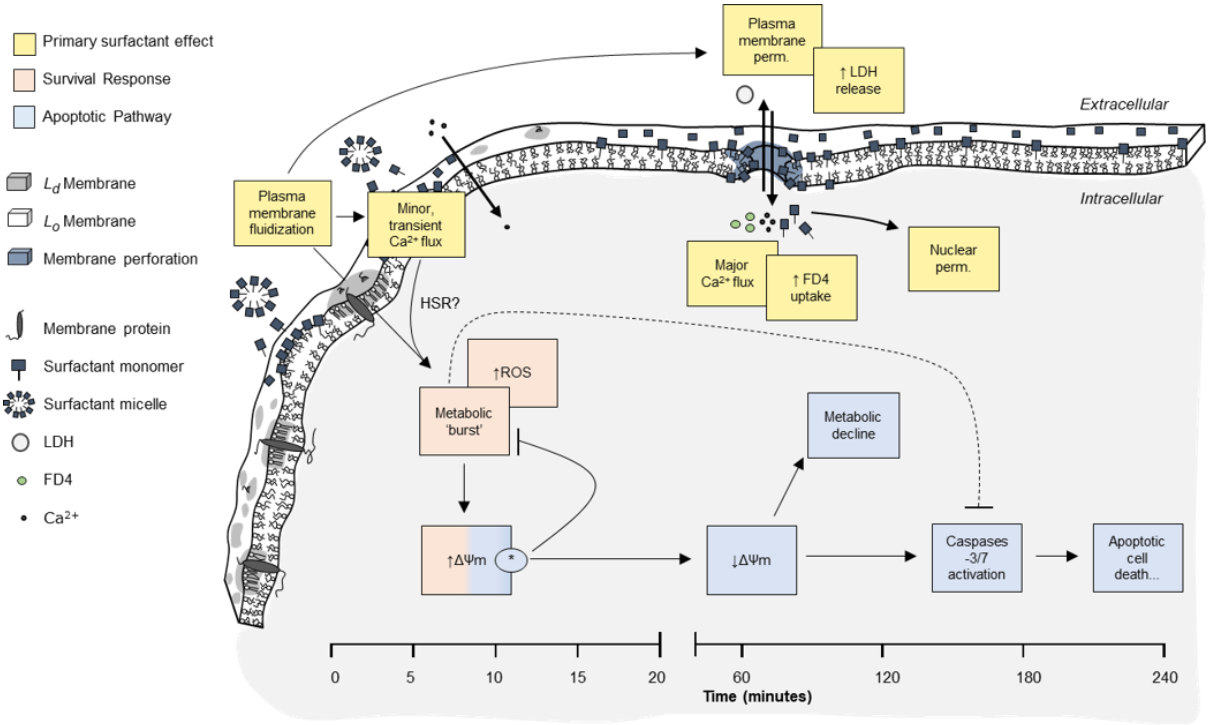

Figure 8. Suggested mechanism of toxicity of high concentrations of non-ionic surfactant on Caco-2 intestinal epithelial cells. Exposure to surfactant includes rapid fluidization of the cell plasma membrane which is associated with minor fluctuations in intracellular Ca^{2+} levels. This could incite a membrane-derived stress response, akin to the heat shock response, and is characterised by an early 'survival' phase (in red) and the subsequent initiation of a stress-induced mitochondrial-mediated apoptotic pathway (in blue). Occurring in parallel to these responses are

the direct membrane effects of surfactant (in yellow) which, over time, progress from stress-inducing disruptions in membrane fluidity, to membrane perturbations associated with increased membrane permeability. LDH, lactose dehydrogenase; FD4, FITC-dextran (4kDa); ΔΨm, mitochondrial membrane potential; perm., permeabilization.

Initial, primary surfactant effects

Changes in the fluorescence profile of the Laurdan probe (Figure 1) indicate the creation of an increasingly hydrophilic, fluid environment within the plasma membrane that occurs immediately upon surfactant application (within 0-1 minute), indicating fast initial incorporation of surfactant molecules into the plasma membrane structure. This initial effect does not appear to induce an immediate increase in membrane permeability, or impairment of plasma membrane barrier function, as judged from the initial absence of FD4 internalization and LDH release (Figure 3b). The transient increase (~10%) in intracellular calcium levels within initial 3 minutes of exposure (Figure 2) is most likely associated with plasma membrane fluidization and associated influx of extracellular calcium (Figure 8).[41]

The initial level of cell membrane fluidization induced by the surfactant (10 mM) within 1 minute of exposure appears comparable in magnitude to that of membrane fluidization of cells exposed to 42°C heat shock (Figure 1e). This similarity suggests that the cells membrane fluidization by the surfactant exposure may be capable of triggering response akin to a mitochondrial heat shock response (Figure 8).[41] In Caco-2 cells, exposure to 42ºC conditions employed in the current study has been previously demonstrated by others to induce heat shock response and expression of associated proteins.[35,36] It should be noted however that in cells exposed to a 42ºC heat shock the Laurdan fluorescence gradually returned to the initial level over time (Figure 1d), unlike in

surfactant exposed counterparts. This apparent recovery of Laurdan GP was unexpected as the 42°C temperature was maintained throughout 2 hours experiment. At this stage, we cannot propose a clear explanation for Laurdan 'recovery' or support the observations with similar literature reports. Possible reasons may include the activation of membrane stabilizing proteins and their opposing effect on the cell membrane fluidization.[42,43]

Changes in cell membrane barrier function, i.e. increased membrane permeability, were manifested later, after ≥60 minutes of exposure to surfactant concentrations ≥1.0 mM, as evidenced by the cell influx and efflux of relatively large molecular weight permeants, FITC-dextran (4 kDa) and LDH enzyme, respectively (Figure 3b). The appearance of the increased permeability coincides approximately with further decrease in Laurdan GP values (between 30-40 minutes; Figure 1c) for surfactant concentrations ≥0.1 mM. The current study corroborates with previous reports,[2,44,45] that increased membrane permeability by non-ionic surfactants the can be associated with surfactant mediated membrane fluidization, but it further reveals that increased membrane fluidity is characterized by an initial (0-1 minute) and secondary stage (>30-40 minutes change in Laurdan polarization, Figure 1b and c), where it is the latter stage of membrane environment change which is responsible for increased permeability. Further studies would be needed to understand how is this time-related phenomenon connected to the non-ionic surfactant molecular structure (Kolliphor HS15), and its consequent trans-bilayer diffusion ('flip-flop') and/or formation of pores in the membrane bilayer.[7,46,47]

Stress-induced survival response

Incorporation of surfactant molecules into, and consequent fluidization of the plasma membrane, have been demonstrated to induce clustering of membrane raft regions;[48] a phenomenon which alters the spatial coordination of membrane proteins involved in cellular thermal sensing and triggers the cellular heat shock response.[49] In addition to this membrane 'restructuring' on surfactant exposure and increased membrane fluidity (Figure 1), the observed transient increase in intracellular calcium (Figure 2) may also play a role in activating the heat shock response; a phenomenon previously observed by others (Figure 8).[41,50,51]

The heat shock response has traditionally been attributed to protein denaturation,[52] however it is now widely established that cellular sensing and responding to stress signals occurs *via* the induction of membrane-associated signalling pathways.[53–55] Due to the nature of its structural molecules, membrane lipid bilayer organization is sensitive to temperature and confers the plasma membrane the ability to act as a 'membrane thermosensor'. The use of non-proteotoxic membrane fluidisers has demonstrated that alterations in membrane fluidity are the first events in the heat sensing pathway;[56] indeed 'membrane fluidisers', such as benzyl alcohol and hydroxylamine derivatives, have been demonstrated to activate the heat shock pathway.[41,57,58] By inference it is possible that the conventional non-ionic surfactant, Kolliphor HS15, can induce the heat shock response in a similar manner to these membrane fluidisers.

Interestingly, a short 5 minutes exposure to ≥1.0 mM surfactant solutions causes a concentration-dependent decrease, relative to control, in effector caspase activation when measured during post-exposure 'recovery' stage (Figure 5b). Thus, short exposure to the surfactant treatment reduces

constitutive apoptosis. This may be related to the heat shock response induced by the surfactant, as caspase inhibition has been recognized as a part of an anti-apoptotic environment and cell survival mechanisms,[59] including a survival response to heat shock (Figure 8).[60,61] In addition, certain heat shock proteins are capable of binding to, and stabilizing heat shock perturbed membranes.[43] This membrane 'stabilization' may be protecting against further surfactant-induced membrane fluidization (between 1-30 minutes, Figure 1) and regulating calcium flux during early exposure times (Figure 2).[62,63] In a similar manner, elements of the heat shock response may be responsible for the decrease in FD4 internalization observed at 5 and 10 minutes (Figure 3), which is further supported by a study conducted by Szöllősi et al. who report a decrease in FITC-dextran internalization in response to heat stress.[64] Thus the activation of the heat shock response may aim / attempt to protect the cell from early lysis by 'consolidating' the membrane and may limit surfactant-induced increase in membrane permeability at early time points by upregulating the membrane stabilizing proteins.[42,43,62,65]

Metabolic effects

The reduction of the MTS tetrazolium salt to a formazan salt is mediated *via* NADH-dependent enzymes.[66] Accordingly, the marked increase in MTS reduction observed at early time points (5 and 10 minutes) on surfactant exposure (≥10.0 mM) probably reflects higher cellular levels of NADH and, consequently, an imbalance in the NADH/NAH+ redox state of cells. To overcome this early redox imbalance, regeneration of NAD+ *via* mitochondrial Complex I (NADH-ubiquinone oxidoreductase) is initiated. NADH oversupply could however overwhelm Complex I,[67] leading to mitochondrial membrane potential *hyperpolarization* and an increase in ROS formation;[68] events consistent with those observed in this study (Figure 4). In fact the observed increase in NADH activity (reflected in MTS reduction) may result from the enhancement of

glycolysis as an element of a survival response, providing energy for rapid cellular adaptation [69] to address the stress stimuli.[70]

Mitochondrial *hyperpolarization* has been suggested to be an early, key signalling element in the heat shock response.[41] Moreover, mitochondrial *hyperpolarization* is recognized as an early step in apoptosis.[39,71] In the present study, it appears that the induction of subsequent effector caspases *via* mitochondrial hyperpolarization is a time-dependent process; the induction of hyperpolarized mitochondria alone does not appear to trigger cell death (0-5 minutes), however its prolonged presence (>5 minutes) does (Figure 8). In support of this idea, our data demonstrate that the inhibition of surfactant induced membrane hyperpolarization by FCCP prevents the activation of caspase 3/7 (Figure 7c).

Stress-induced apoptotic cell death

Our data reveal that exposure to surfactant concentrations above the CMC induce apoptosis, as indicated by effector caspases activation (Figure 5b) and nuclear fragmentation (Figure 6). In addition, unlike the necrotic control (ethanol),[72] surfactant exposure did not induce observable nuclear swelling (Figure 6). These attributes would point to an induction of a form of apoptotic cell death, whereby the observed increases in cell plasma and nuclear membrane permeabilization (Figure 3) are a 'direct' consequences of surfactant action, as opposed to being associated with necrotic processes (Figure 8).

Time course, 'recovery' experiments reveal that the activation of apoptosis appears to occur between 5-10 minutes of surfactant exposure at concentrations ≥ 1.0 mM (Figure 5). Activation of the apoptosis appears to inhibit the cell survival response, as suggested by the sustained metabolic burst that occurs in the absence of mitochondrial hyperpolarization in the presence of FCCP

(Figure 7b); highlighting the potential crosstalk between these pathways.[73] This could be supported by high levels of MTS reduction that continued for almost 180 minutes into the post-exposure 'recovery' (Figure 5a), rather than this metabolic burst subsiding, as seen within 20 minutes in the presence of the surfactant (Fig 4).

The inhibition of apoptosis with FCCP did not however completely prevent mitochondrial membrane potential depolarization, as it was still observed after 180 minutes in the presence of FCCP (Figure 7a). This later depolarization is most likely the consequence of direct surfactant permeabilization of the mitochondrial membranes. Moreover, nuclear membrane permeabilization, which is also evident after ~120 minutes of exposure, was unresponsive to FCCP treatment (Supplementary Figure 10), a feature that indicates permeabilization of this membrane is also occurring as a direct surfactant effect. Both of these phenomena suggest the presence of surfactant molecules in intracellular organelle membranes after prolonged exposure.

How the surfactant molecules access membranes of intracellular organelles remains to be ascertained. Given the amphipathic nature of non-ionic surfactants, their molecules would, according to current understanding, at least initially (Figure 1) accumulate in the plasma membrane. This insertion would (initially) occur into the outer leaflet of the membrane bilayer and, for non-ionic surfactants, the head group appears to strongly influence (if/when) a subsequent trans-bilayer diffusion occurs; estimated half-times ranging from 350 ms to several hours for e.g. octaethylene glycol monododecyl ether and dodecylmaltoside, respectively.[46,74] Beyond plasma membrane incorporation (and effects on its fluidity), a possible contribution to surfactant molecules reaching intracellular membranes could be *via* the normal internalization of damaged membrane sections containing incorporated surfactant by plasma membrane repair mechanisms, as has been observed for membrane injury induced by pore-forming toxins or mechanical force.[75]

A recent study illustrates accumulation of the surfactant molecules in the cell interior *prior* to its lysis, although it should be noticed that the work was conducted using ionic surfactant (sodium dodecyl sulphate).[76] The study proposes that intracellular membrane trafficking contributes to the surfactant uptake mechanism. Non-ionic surfactants have also been demonstrated to interact with, and form channels through lipid membranes *in vitro.*[77] As a consequence, surfactant molecules may diffuse though created pores (Figure 8), an event that would occur at latter times and higher surfactant concentrations, as potentially indicated by later influx of FD4 and LDH leakage (Figure 3).

Finally, one could view apoptotic cell death as actually conferring protection to the cell population, or tissue as a whole, from surfactant-induced immunogenicity. The loss of cell membrane barrier function, and the consequent leakage of intracellular components, will likely promote immunogenic response in the surrounding cells and tissue.[78,79] The induction of *rapid* mitochondrially-mediated apoptosis can thus be viewed as advantageous, as it might minimize the toxic potential of surfactant exposure.

Conclusions

The primary observation of this study is that cell membrane fluidization caused by exposure to non-ionic surfactant is a process akin to thermal stress, resulting in the cellular heat shock response. This has a relevance to the behaviour of other non-ionic surfactants used in therapeutic formulations, such as the alkylglycosides[2,44] and polysorbates,[45] which have been suggested to mediate their increases in cell membrane permeability *via* the induction of membrane fluidization. Taken together, our data suggest that the safe use of non-ionic surfactants which operate by such

a mechanism may be limited by the fact that their membrane permeability action is intrinsically linked to alterations in membrane fluidity and, an induction of apoptotic cell death. The work performed here therefore provides a foundation from which the study of other non-ionic surfactants could be furthered. Similarly, the findings reported here on intestinal epithelium may be applicable to permeability studies performed on other epithelial layers, such as airway epithelium.

Our study indicates that non-ionic surfactant cytotoxicity is induced by membrane effects, however, it is the mitochondrial function and mitochondria associated responses, that are consequently triggered, that in fact mediate the majority of observed cytotoxicity, not membrane perturbations *per se*. This novel finding, arising from the time-course studies, may inform the way the toxicity of surfactants and other amphipathic compounds are evaluated.

Acknowledgements

This work was funded by the Medical Research Council (MRC) Grant number 1872576.

Conflicts of Interests

The authors declare they have no conflicts of interest.

Author Contributions

R.C. acquired and analysed the data and drafted the manuscript; P.S. provided the expertise for the calcium imaging and performed the statistical analysis. R.C.; P.S.; S.S. participated in revising the manuscript; S.S. obtained funding for the study and drafted the manuscript.

Supporting Information

Optimisation of Triton X-100, Valinomycin, Staurosporine and FCCP concentrations used in the study. Intracellular Ca^{2+} levels over 120 minutes of exposure. Fluorescent cellular images of CellTox Green dye. ROS levels detected with CM-H2DCFDA probe following cell incubation with H_2O_2 (positive control). Metabolic activity measured with PrestoBlue reagent, and mitochondrial membrane potential assessed with Mitotracker Red probe. Effect of FCCP (0.5 μM) and Kolliphor HS15 exposure on ROS and CellTox Green assay results.

References

(1) Dimitrijevic, D.; Shaw, A. J.; Florence, A. T. Effects of Some Non-Ionic Surfactants on Transepithelial Permeability in Caco-2 Cells. *J. Pharm. Pharmacol.* **2000**, *52*, 157–162.

(2) Vllasaliu, D.; Shubber, S.; Fowler, R.; Garnett, M.; Alexander, C.; Stolnik, S. Epithelial Toxicity of Alkylglycoside Surfactants. *J. Pharm. Sci.* **2013**, *102*, 114–125.

(3) Kiss, L.; Walter, F. R.; Bocsik, A.; Veszelka, S.; Ozsvari, B.; Puskas, L. G.; Szabo-Revesz, P.; Deli, M. A. Kinetic Analysis of the Toxicity of Pharmaceutical Excipients Cremophor EL and RH40 on Endothelial and Epithelial Cells. *J. Pharm. Sci.* **2013**, *102*, 1173–1181.

(4) Aungst, B. J. Absorption Enhancers: Applications and Advances. *The AAPS Journal*. 2012, pp 10–18.

(5) Arnold, J. .; Ahsan, F.; Meezen, E.; Pillion, D. . Correlation of Tetradecylmaltoside Induced Increases in Nasal Peptide Drug Delivery with Morphological Changes in Nasal Epithelial Cells. *J. Pharm. Sci.* **2004**, *93*, 2205–2213.

(6) Calvello, R.; Mitolo, V.; Acquafredda, A.; Cianciulli, A.; Panaro, M. A. Plasma Membrane Damage Sensing and Repairing. Role of Heterotrimeric G-Proteins and the Cytoskeleton. *Toxicol. Vitr.* **2011**, *25*, 1067–1074.

(7) Groot, R. D.; Rabone, K. L. Mesoscopic Simulation of Cell Membrane Damage, Morphology Change and Rupture by Nonionic Surfactants. *Biophys. J.* **2001**, *81*, 725–736.

(8) Alani, A.; Rao, D.; Seidel, R. The Effect of Novel Surfactants and Solutol® HS 15 on Paclitaxel Aqueous Solubility and Permeability across a Caco-2 Monolayer. *J. Pharm. Sci.* **2010**, *99* (8), 3473–3485.

(9) Kiss, L.; Hellinger, É.; Pilbat, A.-M.; Kittel, Á.; Török, Z.; Füredi, A.; Szakács, G.; Veszelka, S.; Sipos, P.; Ózsvári, B.; et al. Sucrose Esters Increase Drug Penetration, But Do Not Inhibit P-Glycoprotein in Caco-2 Intestinal Epithelial Cells. *J. Pharm. Sci.* **2014**, *103* (10), 3107–3119.

(10) Yamaguchi, J. Y.; Nishimura, Y.; Kanada, A.; Kobayashi, M.; Mishima, K.; Tatsuishi, T.; Iwase, K.; Oyama, Y. Cremophor EL, a Non-Ionic Surfactant, Promotes Ca2+-Dependent Process of Cell Death in Rat Thymocytes. *Toxicology* **2005**, *211* (3), 179–186.

(11) Yang, Y. W.; Wu, C. a.; Morrow, W. J. W. Cell Death Induced by Vaccine Adjuvants Containing Surfactants. *Vaccine* **2004**, *22* (11–12), 1524–1536.

(12) Eskandani, M.; Hamishehkar, H.; Ezzati Nazhad Dolatabadi, J. Cyto/Genotoxicity Study of Polyoxyethylene (20) Sorbitan Monolaurate (Tween 20). *DNA Cell Biol.* **2013**, *32* (9), 498–503.

(13) Gan, L.; Gan, Y.; Zhu, C.; Zhang, X.; Zhu, J. Novel Microemulsion in Situ Electrolyte-Triggered Gelling System for Ophthalmic Delivery of Lipophilic Cyclosporine A: In Vitro and in Vivo Results. *Int. J. Pharm.* **2009**, *365* (1–2), 143–149.

(14) Mao, C.; Wan, J.; Chen, H.; Xu, H.; Yang, X. Emulsifiers' Composition Modulates Venous Irritation of the Nanoemulsions as a Lipophilic and Venous Irritant Drug Delivery System. *AAPS PharmSciTech* **2009**, *10* (3), 1058–1064.

(15) Vonarbourg, A.; Passirani, C.; Desigaux, L.; Allard, E.; Saulnier, P.; Lambert, O.; Benoit, J. P.; Pitard, B. The Encapsulation of DNA Molecules within Biomimetic Lipid Nanocapsules. *Biomaterials* **2009**, *30* (18), 3197–3204.

(16) Zhou, T.; Zhu, L.; Xia, H.; He, J.; Liu, S.; He, S.; Wang, L.; Zhang, J. Micelle Carriers Based on Macrogol 15 Hydroxystearate for Ocular Delivery of Terbinafine Hydrochloride: In Vitro Characterization and in Vivo Permeation. *Eur. J. Pharm. Sci.* **2017**, *109*, 288–296.

(17) Illum, L.; Jordan, F.; Lewis, A. L. CriticalSorb: A Novel Efficient Nasal Delivery System for Human Growth Hormone Based on Solutol HS15. *J. Control. Release* **2012**, *162* (1), 194–200.

(18) Brayden, D. J.; Bzik, V. a; Lewis, a L.; Illum, L. CriticalSorb™ Promotes Permeation of Flux Markers across Isolated Rat Intestinal Mucosae and Caco-2 Monolayers. *Pharm. Res.* **2012**, *29* (9), 2543–2554.

(19) Lewis, A. L.; Jordan, F.; Illum, L. CriticalSorb(TM): Enabling Systemic Delivery of Macromolecules via the Nasal Route. *Drug Deliv. Transl. Res.* **2013**, *3* (1), 26–32.

(20) Cornaire, G.; Woodley, J.; Hermann, P.; Cloarec, A.; Arellano, C.; Houin, G. Impact of Excipients on the Absorption of P-Glycoprotein Substrates in Vitro and in Vivo. *Int. J. Pharm.* **2004**, *278* (1), 119–131.

(21) Shubber, S.; Vllasaliu, D.; Rauch, C.; Jordan, F.; Illum, L.; Stolnik, S. Mechanism of Mucosal Permeability Enhancement of CriticalSorb® (Solutol® HS15) Investigated In Vitro in Cell Cultures. *Pharm. Res.* **2014**, *32* (2), 516–527.

(22) Arnold, J. J.; Ahsan, F.; Meezan, E.; Pillion, D. J. Correlation of Tetradecylmaltoside Induced Increases in Nasal Peptide Drug Delivery with Morphological Changes in Nasal Epithelial Cells. *J. Pharm. Sci.* **2004**, *93* (9), 2205–2213.

(23) McCartney, F.; Gleeson, J. P.; Brayden, D. J. Safety Concerns over the Use of Intestinal Permeation Enhancers: A Mini-Review. *Tissue Barriers*. 2016.

(24) Parasassi, T.; De Stasio, G.; Ravagnan, G.; Rusch, R. M.; Gratton, E. Quantitation of Lipid Phases in Phospholipid Vesicles by the Generalized Polarization of Laurdan Fluorescence. *Biophys. J.* **1991**, *60* (1), 179–189.

(25) Vaslin, A.; Puyal, J.; Borsello, T.; Clarke, P. G. H. Excitotoxicity-Related Endocytosis in Cortical Neurons. *J. Neurochem.* **2007**, *102* (3), 789–800.

(26) Navone, S. E.; Marfia, G.; Invernici, G.; Cristini, S.; Nava, S.; Balbi, S.; Sangiorgi, S.; Ciusani, E.; Bosutti, A.; Alessandri, G.; et al. Isolation and Expansion of Human and Mouse Brain Microvascular Endothelial Cells. *Nat. Protoc.* **2013**, *8* (9), 1680–1693.

(27) Reers, M.; Smith, T. W.; Chen, L. B. J-Aggregate Formation of a Carbocyanine as a Quantitative Fluorescent Indicator of Membrane Potential. *Biochemistry* **1991**, *30* (18),

4480–4486.

(28) Perelman, A.; Wachtel, C.; Cohen, M.; Haupt, S.; Shapiro, H.; Tzur, A. JC-1: Alternative Excitation Wavelengths Facilitate Mitochondrial Membrane Potential Cytometry. *Cell Death Dis.* **2012**, *3* (11), e430.

(29) Carpentier, R.; Platel, A.; Maiz-Gregores, H.; Nesslany, F.; Betbeder, D. Vectorization by Nanoparticles Decreases the Overall Toxicity of Airborne Pollutants. *PLoS One* **2017**, *12* (8).

(30) Suzuki, T.; Fujikura, K.; Higashiyama, T.; Takata, K. DNA Staining for Fluorescence and Laser Confocal Microscopy. *J. Histochem. Cytochem.* **1997**, *45* (1), 49–53.

(31) Nishikawa, T.; Edelstein, D.; Du, X. L.; Yamagishi, S. I.; Matsumura, T.; Kaneda, Y.; Yorek, M. A.; Beebe, D.; Oates, P. J.; Hammes, H. P.; et al. Normalizing Mitochondrial Superoxide Production Blocks Three Pathways of Hyperglycaemic Damage. *Nature* **2000**, *404* (6779), 787–790.

(32) Metkar, S. S.; Wang, B.; Catalan, E.; Anderluh, G.; Gilbert, R. J. C.; Pardo, J.; Froelich, C. J. Perforin Rapidly Induces Plasma Membrane Phospholipid Flip-Flop. *PLoS One* **2011**, *6* (9).

(33) Bentley, D. C.; Pulbutr, P.; Chan, S.; Smith, P. A. Etiology of the Membrane Potential of Rat White Fat Adipocytes. *AJP Endocrinol. Metab.* **2014**, *307*, E161–E175.

(34) Verstraeten, S. V.; Jaggers, G. K.; Fraga, C. G.; Oteiza, P. I. Procyanidins Can Interact with Caco-2 Cell Membrane Lipid Rafts: Involvement of Cholesterol. *Biochim. Biophys. Acta - Biomembr.* **2013**, *1828* (11), 2646–2653.

(35) Malago, J. J.; Koninkx, J. F. J. G.; Ovelgönne, H. H.; van Asten, F. J. a M.; Swennenhuis, J. F.; van Dijk, J. E. Expression Levels of Heat Shock Proteins in Enterocyte-like Caco-2 Cells after Exposure to Salmonella Enteritidis. *Cell Stress Chaperones* **2003**, *8* (2), 194–203.

(36) Phanvijhitsiri, K.; Musch, M. W.; Ropeleski, M. J.; Chang, E. B. Heat Induction of Heat Shock Protein 25 Requires Cellular Glutamine in Intestinal Epithelial Cells. *Am. J. Physiol. Cell Physiol.* **2006**, *291* (2), C290-9.

(37) Belmokhtar, C. A.; Hillion, J.; Ségal-Bendirdjian, E. Staurosporine Induces Apoptosis through Both Caspase-Dependent and Caspase-Independent Mechanisms. *Oncogene* **2001**, *20* (26), 3354–3362.

(38) Stoetzer, O. J.; Pogrebniak, A.; Pelka-Fleischer, R.; Hasmann, M.; Hiddemann, W.; Nuessler, V. Modulation of Apoptosis by Mitochondrial Uncouplers: Apoptosis-Delaying Features despite Intrinsic Cytotoxicity. *Biochem. Pharmacol.* **2002**, *63* (3), 471–483.

(39) Giovannini, C.; Matarrese, P.; Scazzocchio, B.; Sanchez, M.; Masella, R.; Malorni, W. Mitochondria Hyperpolarization Is an Early Event in Oxidized Low-Density Lipoprotein-Induced Apoptosis in Caco-2 Intestinal Cells. *FEBS Lett.* **2002**, *523* (1–3), 200–206.

(40) Koley, D.; Bard, A. J. Triton X-100 Concentration Effects on Membrane Permeability of a Single HeLa Cell by Scanning Electrochemical Microscopy (SECM). *Proc. Natl. Acad. Sci. U. S. A.* **2010**, *107* (39), 16783–16787.

(41) Balogh, G.; Horváth, I.; Nagy, E.; Hoyk, Z.; Benkõ, S.; Bensaude, O.; Vígh, L. The Hyperfluidization of Mammalian Cell Membranes Acts as a Signal to Initiate the Heat Shock Protein Response. *FEBS J.* **2005**, *272* (23), 6077–6086.

(42) Torok, Z.; Horvath, I.; Goloubinoff, P.; Kovacs, E.; Glatz, A.; Balogh, G.; Vigh, L.

Evidence for a Lipochaperonin: Association of Active Proteinfolding GroESL Oligomers with Lipids Can Stabilize Membranes under Heat Shock Conditions. *Proc. Natl. Acad. Sci.* **1997**, *94* (6), 2192–2197.

(43) Török, Z.; Goloubinoff, P.; Horváth, I.; Tsvetkova, N. M.; Glatz, a; Balogh, G.; Varvasovszki, V.; Los, D. a; Vierling, E.; Crowe, J. H.; et al. Synechocystis HSP17 Is an Amphitropic Protein That Stabilizes Heat-Stressed Membranes and Binds Denatured Proteins for Subsequent Chaperone-Mediated Refolding. *Proc. Natl. Acad. Sci. U. S. A.* **2001**, *98*, 3098–3103.

(44) Petersen, S. B.; Nolan, G.; Maher, S.; Rahbek, U. L.; Guldbrandt, M.; Brayden, D. J. Evaluation of Alkylmaltosides as Intestinal Permeation Enhancers: Comparison between Rat Intestinal Mucosal Sheets and Caco-2 Monolayers. *Eur. J. Pharm. Sci.* **2012**, *47* (4), 701–712.

(45) Rege, B. D.; Kao, J. P. Y.; Polli, J. E. Effects of Nonionic Surfactants on Membrane Transporters in Caco-2 Cell Monolayers. *Eur. J. Pharm. Sci.* **2002**, *16* (4–5), 237–246.

(46) Kragh-Hansen, U.; le Maire, M.; Møller, J. V. The Mechanism of Detergent Solubilization of Liposomes and Protein-Containing Membranes. *Biophys. J.* **1998**, *75* (6), 2932–2946.

(47) Xia, W. J.; Onyuksel, H. Mechanistic Studies on Surfactant-Induced Membrane Permeability Enhancement. *Pharm. Res.* **2000**, *17* (5), 612–618.

(48) Fine, M.; Llaguno, M. C.; Lariccia, V.; Lin, M.-J.; Yaradanakul, A.; Hilgemann, D. W. Massive Endocytosis Driven by Lipidic Forces Originating in the Outer Plasmalemmal Monolayer: A New Approach to Membrane Recycling and Lipid Domains. *J. Gen. Physiol.* **2011**, *137* (2), 137–154.

(49) Vigh, L.; Escribá, P. V.; Sonnleitner, A.; Sonnleitner, M.; Piotto, S.; Maresca, B.; Horváth, I.; Harwood, J. L. The Significance of Lipid Composition for Membrane Activity: New Concepts and Ways of Assessing Function. *Progress in Lipid Research*. 2005, pp 303–344.

(50) Price, B. D.; Calderwood, S. K. Ca2+ Is Essential for Multistep Activation of the Heat Shock Factor in Permeabilized Cells. *Mol. Cell. Biol.* **1991**, *11* (6), 3365–3368.

(51) Choi; Tucker; Carlson; Weigand; Holbrook. Calcium Mediates Expression of Stress-Response Genes in Prostaglandin A2-Induced Growth Arrest. *FASEB J* **1994**, *8* (13), 1048–1054.

(52) Hightower, L. E.; White, F. P. Cellular Responses to Stress: Comparison of a Family of 71–73-kilodalton Proteins Rapidly Synthesized in Rat Tissue Slices and Canavanine-treated Cells in Culture. *J. Cell. Physiol.* **1981**, *108* (2), 261–275.

(53) Vigh, L.; Maresca, B.; Harwood, J. L. Does the Membrane's Physical State Control the Expression of Heat Shock and Other Genes? *Trends Biochem. Sci.* **1998**, *23* (10), 369–374.

(54) Parton, R. G.; del Pozo, M. A. Caveolae as Plasma Membrane Sensors, Protectors and Organizers. *Nat. Rev. Mol. Cell Biol.* **2013**, *14* (2), 98–112.

(55) Berchtold, D.; Piccolis, M.; Chiaruttini, N.; Riezman, I.; Riezman, H.; Roux, A.; Walther, T. C.; Loewith, R. Plasma Membrane Stress Induces Relocalization of Slm Proteins and Activation of TORC2 to Promote Sphingolipid Synthesis. TL - 14. *Nat. Cell Biol.* **2012**, *14 VN-r* (5), 542–547.

(56) Vigh, L.; Török, Z.; Crul, T.; Maresca, B.; Schütz, G. J.; Viana, F.; Dindia, L.; Piotto, S.; Brameshuber, M.; Balogh, G.; et al. Plasma Membranes as Heat Stress Sensors: From Lipid-Controlled Molecular Switches to Therapeutic Applications. *Biochimica et Biophysica Acta*

- *Biomembranes*. 2014, pp 1594–1618.

(57) Vígh, L.; Literáti, P. N.; Horváth, I.; Török, Z.; Balogh, G.; Glatz, a; Kovács, E.; Boros, I.; Ferdinándy, P.; Farkas, B.; et al. Bimoclomol: A Nontoxic, Hydroxylamine Derivative with Stress Protein-Inducing Activity and Cytoprotective Effects. *Nat. Med.* **1997**, *3* (10), 1150–1154.

(58) Török, Z.; Tsvetkova, N. M.; Balogh, G.; Horváth, I.; Nagy, E.; Pénzes, Z.; Hargitai, J.; Bensaude, O.; Csermely, P.; Crowe, J. H.; et al. Heat Shock Protein Coinducers with No Effect on Protein Denaturation Specifically Modulate the Membrane Lipid Phase. *Proc. Natl. Acad. Sci. U. S. A.* **2003**, *100* (6), 3131–3136.

(59) Portt, L.; Norman, G.; Clapp, C.; Greenwood, M.; Greenwood, M. T. Anti-Apoptosis and Cell Survival: A Review. *Biochimica et Biophysica Acta - Molecular Cell Research*. 2011, pp 238–259.

(60) Bruey, J. M.; Ducasse, C.; Bonniaud, P.; Ravagnan, L.; Susin, S. A.; Diaz-Latoud, C.; Gurbuxani, S.; Arrigo, A. P.; Kroemer, G.; Solary, E.; et al. Hsp27 Negatively Regulates Cell Death by Interacting with Cytochrome C. *Nat. Cell Biol.* **2000**, *2* (9), 645–652.

(61) Pandey, P.; Farber, R.; Nakazawa, a; Kumar, S.; Bharti, a; Nalin, C.; Weichselbaum, R.; Kufe, D.; Kharbanda, S. Hsp27 Functions as a Negative Regulator of Cytochrome c-Dependent Activation of Procaspase-3. *Oncogene* **2000**, *19* (16), 1975–1981.

(62) Tsvetkova, N. M.; Horvath, I.; Torok, Z.; Wolkers, W. F.; Balogi, Z.; Shigapova, N.; Crowe, L. M.; Tablin, F.; Vierling, E.; Crowe, J. H.; et al. Small Heat-Shock Proteins Regulate Membrane Lipid Polymorphism. *Proc Natl Acad Sci U S A* **2002**, *99* (21), 13504–13509.

(63) Horváth, I.; Glatz, a; Varvasovszki, V.; Török, Z.; Páli, T.; Balogh, G.; Kovács, E.; Nádasdi, L.; Benkö, S.; Joó, F.; et al. Membrane Physical State Controls the Signaling Mechanism of the Heat Shock Response in Synechocystis PCC 6803: Identification of hsp17 as A "fluidity Gene". *Proc. Natl. Acad. Sci. U. S. A.* **1998**, *95* (7), 3513–3518.

(64) Szöllősi, A. G.; Oláh, A.; Tóth, I. B.; Papp, F.; Czifra, G.; Panyi, G.; Bíró, T. Transient Receptor Potential Vanilloid-2 Mediates the Effects of Transient Heat Shock on Endocytosis of Human Monocyte-Derived Dendritic Cells. *FEBS Lett.* **2013**, *587* (9), 1440–1445.

(65) Horváth, I.; Multhoff, G.; Sonnleitner, A.; Vígh, L. Membrane-Associated Stress Proteins: More than Simply Chaperones. *Biochimica et Biophysica Acta - Biomembranes*. 2008, pp 1653–1664.

(66) Berridge, M. V.; Herst, P. M.; Tan, A. S. Tetrazolium Dyes as Tools in Cell Biology: New Insights into Their Cellular Reduction. *Biotechnology Annual Review*. 2005, pp 127–152.

(67) He, Q.; Wang, M.; Petucci, C.; Gardell, S. J.; Han, X. Rotenone Induces Reductive Stress and Triacylglycerol Deposition in C2C12 Cells. *Int. J. Biochem. Cell Biol.* **2013**, *45* (12), 2749–2755.

(68) Starkov, A. A.; Fiskum, G. Regulation of Brain Mitochondrial H2O2 Production by Membrane Potential and NAD(P)H Redox State. *J. Neurochem.* **2003**, *86* (5), 1101–1107.

(69) Bolaños, J. P.; Almeida, A.; Moncada, S. Glycolysis: A Bioenergetic or a Survival Pathway? *Trends in Biochemical Sciences*. 2010, pp 145–149.

(70) Fulda, S.; Gorman, A. M.; Hori, O.; Samali, A. Cellular Stress Responses: Cell Survival and Cell Death. *International Journal of Cell Biology*. 2010.

(71) Sánchez-Alcázar, J.; Ault, J.; Khodjakov, A.; Schneider, E. Increased Mitochondrial

Cytochrome c Levels and Mitochondrial Hyperpolarization Precede Camptothecin-Induced Apoptosis in Jurkat Cells. *Cell Death Differ.* **2000**, *7* (11), 1090–1100.

(72) Hoek, J. B.; Cahill, A.; Pastorino, J. G. Alcohol and Mitochondria: A Dysfunctional Relationship. *Gastroenterology* **2002**, *122* (7), 2049–2063.

(73) Vanden Berghe, T.; Kaiser, W. J.; Bertrand, M. J.; Vandenabeele, P. Molecular Crosstalk between Apoptosis, Necroptosis, and Survival Signaling. *Mol. Cell. Oncol.* **2015**, *2* (4), e975093.

(74) le Maire, M.; Moller, J. V.; Champeil, P. Binding of a Nonionic Detergent to Membranes: Flip-Flop Rate and Location on the Bilayer. *Biochemistry* **1987**, *26* (15), 4803–4810.

(75) Corrotte, M.; Almeida, P. E.; Tam, C.; Castro-Gomes, T.; Fernandes, M. C.; Millis, B. A.; Cortez, M.; Miller, H.; Song, W.; Maugel, T. K.; et al. Caveolae Internalization Repairs Wounded Cells and Muscle Fibers. *Elife* **2013**, *2013* (2).

(76) Okuno, M.; Kano, H.; Fujii, K.; Bito, K.; Naito, S.; Leproux, P.; Couderc, V.; Hamaguchi, H. O. Surfactant Uptake Dynamics in Mammalian Cells Elucidated with Quantitative Coherent Anti-Stokes Raman Scattering Microspectroscopy. *PLoS One* **2014**, *9* (4).

(77) Schlieper, P.; de Roberts, E. Triton X-100 as a Channel-Forming Substance in Artificial Lipid Bilayer Membranes. *Arch. Biochem. Biophys.* **1977**, *184*, 204–208.

(78) Thompson, C. B. Apoptosis in the Pathogenesis and Treatment of Disease. *Science* **1995**, *267* (5203), 1456–1462.

(79) Green, D. R.; Ferguson, T.; Zitvogel, L.; Kroemer, G. Immunogenic and Tolerogenic Cell Death. *Nat. Rev. Immunol.* **2009**, *9* (5), 353–363.

For Table of Contents Use Only

Exposure to a non-ionic surfactant induces a response akin to heat-shock apoptosis in intestinal epithelial cells: implications for excipients safety

Robert J. Cavanagh, Paul A. Smith and Snow Stolnik